Available online at www.sciencedirect.com

ScienceDirect

Procedia CIRP 50 (2016) 94 – 99

www.elsevier.com/locate/procedia

26th CIRP Design Conference

Finite Element Analysis and Validation of Cellular Structures

Mark Helou[a,*], Supachai Vongbunyong[b], Sami Kara[a]

[a]*Sustainable Manufacturing and Life Cycle Engineering Research Group, The University of New South Wales, Australia*
[b]*Institute of Field Robotics, King Mongkut's University of Technology Thonburi, Thailand*

[*] Corresponding author. Tel.: +61 (2)-9933-3666; fax: +61 (2)-9933-3699. *E-mail address:* mark.helou@breseight.com.au

Abstract

Additive manufacturing has opened doors to many new technological developments that could not be realised with traditional manufacturing methods. One of these research areas includes the development and utilisation of Cellular Structures in everyday objects. The application of cellular structures theoretically should decrease the required amount of material for production at the cost of overall rigidity and resistance to stresses. This article presents a validation of Finite Element Analysis (FEA) simulations of Cellular Structures with empirical data obtained from compression tests. Parametrised cells with two different materials are evaluated through FEA simulations against selective laser sintered specimens. The cellular structure are modelled with implicit modelling method.

Peer-review under responsibility of the organizing committee of the 26th CIRP Design Conference

Keywords: Cellular Structure, Finite Element Analysis, Additive Manufacturing

1. Introduction

1.1. Overview of Cellular Structures

As additive manufacturing is a growing technology, various efforts have been made to research and develop ways to increase the efficiency of production. Some research has been put into performance improvements in the sintering process by optimising laser wavelengths for faster building speed and creating more accurate lasers [1], as well as minimising the amount of material utilised while manufacturing. There is a growing field within manufacturing that aims to reduce the amount of material used in the manufacturing process, theoretically maintaining or even increasing the amount of strength of the object with a reduction in weight [2]; aptly named Cellular Design, which is of direct interest to this project and will thus be the main research area.

Cellular Design is a process where an object is designed to be created through the additive manufacturing process by building layers of cellular structures upon themselves until the final product is produced. A cellular structure is an object that can be manufactured from materials of varying densities [3], possessing internal micro structures that reinforce and strengthen the object. Essentially, they are the utilisation of periodically repeating unit cells that interconnect in three dimensions. Cellular structures can thus be ultimately defined as objects that possess internal symmetrical geometric micro-structures that are much smaller than the overall size.

These 3D structures are intended to utilise existing structures in nature [4], imitating geometric structures such as honeycombs, cork, porous bone structure and trusses in order to utilise their benefits. The lattice structures utilise tessellating cells to fill a desired volume; they can be created from any form of repeating pattern as long as they interconnect in three dimensions.

Each unit cell is essentially described by three parameters dictating its volume; (a) length, (b) width and (c) height. Because it is extremely important to create a repeatable cell, the parameters are usually made equal to each other to create a unit cube to ensure that a significant amount of shapes can be filled with tessellations and variations of the cell. However, since each parameter could potentially be modified individually, the definition of a cellular structure becomes extremely broad in the sense that any structure that can be identified to be comprised of a tessellated single cell can be counted as a cellular structure. Thus, in this study, the definition of a cellular structure is restricted to a basic unit cube on a meso-scale size (between 0.1 to 10 mm).

1.2. Design and Manufacturing

A significant benefit of the utilisation of cellular structures is that it is superior to traditional methods of subtractive manufacturing due to the reduced requirement of material, time, and energy. Because cellular designs feature large voids within and in-between cells, there can be a significant reduction of utilised material because there is no material loss due to subtractive manufacturing methods such as milling or lathing [5]. They consume less time to produce as opposed to solid designs as

Peer-review under responsibility of the organizing committee of the 26th CIRP Design Conference
doi:10.1016/j.procir.2016.05.018

there is less material required to sinter in the DSLS and DSLM methods [2]. Significant amount of energy consumption reduces directly dependant on the surface area being laser sintered when compared to sintering a solid block of identical volume [6].

The cellular structure design is especially important in application due to its inherent high performance nature - producing very high strength designs with relatively low mass. They also are extremely good at energy and shock absorption, as well as well as being good thermal and acoustic insulators [7]. Although the technology to manufacture structures at the mesoscale and the microscale is increasingly becoming more advanced, there is an extremely large separation between traditional design and more advanced design that takes advantage of the additive manufacturing technologies such as SLS and SLM. There is a distinct lack of a rule of thumb during the design of cellular structures, which in turn causes a portfolio of existing cellular structures to be lacking, hampering the amount of structures that can be implemented.

1.3. Cellular Structure Generation

Existing methods of cellular structure generation typically utilise a manual editing of geometry to achieve the final product. The procedure of creating a structure is usually automated [8], wherein the ends of the unit cell have their faces removed and then are joined via a boolean technique with other cells to create a larger structure. This technique is also utilised in creating different cellular structure types [9], utilising cylinders and polyhedral geometric shapes to form innovative designs. These recreation methods are various and well defined, however many manual short cuts are taken in order to achieve a final product, including repairs to geometrical errors by applying spherical junction at each node to smooth the connection and strengthen the structure as it was built [9]. There exists also an innovative concept of Prefabrication Hybrid Geometry Modeling (P-HGM) [10,11] that rapidly generates the cellular structure with boundary representation (B-Rep) and polygonal surface format, STL.

The utilisation of implicit functions was introduced and results in a much better performing structure in compression testing [2]. The utilisation of implicit functions such as triply periodic minimal surfaces become popular due to their ease of manufacturability and the ability to change structure generation parameters in order to achieve optimal structure design for the intended purpose [12].

1.4. FEA on Cellular Structures

Although there is a large amount of research conducted on the generation of cellular structures, there is surprisingly little regarding the simulation of such structures using Finite Element Analysis (FEA). The aim of this study is to explore the behaviour of FEA simulations conducted on cellular structure specimens via inverse testing, utilising data recorded from empirical compression tests. Due to the extremely large cost associated with rapid prototyping of projects for design verification and testing, there is a need to utilise Finite Element Simulation in order to predict the behaviour of the device featuring cellular structure design in order to reduce lead time in manufacturing as well as decrease the overall cost of manufacturing a prototype utilising advanced manufacturing machinery.

A significant amount of variance between empirical results and simulation data has been found repeatedly between a variety of studies which provide evidence of a cumulative error caused in different stages of the experiment procedure. [13] show that there is a significant error between the experimental and theoretical elastic modulus of Nylon-12, whereas [14] demonstrate that there is a significant error between a numerical analysis simulation and traditional FEA modelling in SLS due to the inability to describe the porosity of the sintered material in traditional FEA products.

However, the behaviour of selective laser sintered products has not been examined in detail when they are applied to the manufacturing of cellular structures. This study aims to verify and further investigate the sources of errors in the FEA simulation of cellular structures by using a range of cellular structure types and examine the reasons of failure.

1.5. Organization of this Paper

This paper outlines as follow. The generation of cellular structures, FEA, and manufacturing point of view are in Section 2. Experiments design and result are in Section 3. Discussion and conclusion of this work are presented in Section 4-5.

2. Methodology

2.1. Generation and Manufacturing

In this study, a comparison between simulated and empirical compression tests are undertaken in order to compare the difference between of SLS cellular structure blocks in reality and FEA. To conduct FEA on the cellular structures, they must first be modelled using approximations that accurately represent the family of structures. Once a representation is created, finite element modelling can be undertaken by applying approximations to the empirical testing scheme in order to generate data that can be compared.

The cellular structures, once generated, will be manufactured by using SLS and SLM. The SLS method sinters each atomised particle of the powder together at each edge, unlike the SLM method which melts the powder into surrounding powder to form a mostly uniform object layer.

2.2. Modelling method generation of cellular structure

To generate each cellular structure, a building block, or unit cell, has to be created as a seed for the final cube. Each triply periodic minimalistic surface type that was to be utilised was created with a trigonometric approximation. All solid files were generated in MATLAB 8.5 [15], utilising a variety of parameters to create each cellular structure seed block through their given equations. Two parameters - (a) the thickness of the cell walls and (b) the seed unit cell length - can be varied in order to characterise the cellular structure.

The three different cellular structure types - namely Schoen Gyroid, Diamond, and Neovius (see Fig. 1) - are designed and produced to compare theoretical simulation and mechanical testing results. The equations used for formulating the Schoen

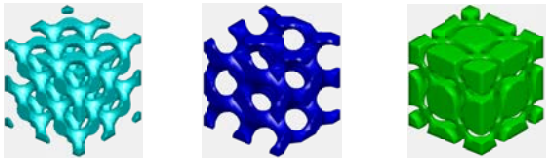

(a) Diamond (b) Gyroid (c) Neovius

Fig. 1: Types of TPMS cellular structure generated in MATLAB

Gyroid, Diamond and Neovius cellular structures structures are Eq. (1)-(3) respectivley. The overall cube size of the samples is limited to 20mm x 20mm x 26mm, according to the limitation of the machine (EOS p380 and m270).

$$F(X,Y,Z) = \cos(X)\,\sin(Y) + \cos(Z)\,\sin(X) + \cos(Y)\,\sin(Z) \quad (1)$$

$$F(X,Y,Z) = \sin(X)\sin(Y)\sin(Z) + \sin(X)\cos(Y)\cos(Z) + \cos(X)\sin(Y)\cos(Z) + \cos(X)\cos(Y)\sin(Z) \quad (2)$$

$$F(X,Y,Z) = 3 * (\cos(X) + \cos(Y) + \cos(Z)) + 4 * (\cos(X)\cos(Y)\cos(Z)) \quad (3)$$

The MATLAB produced STL files have a variety of issues that would affect the geometry when interpreted by other software. The issues, including (a) direction of normal vector cannot be specified and (b) triangle intersection exists, ultimately lead to validity and manufacturability. As a result, the geometry of the generated structures needs to be repaired before they can be manufactured.

STL format represents geometry in the form of 3D facets which is a surface model, while FEA needs to apply on solid model of the geometry. Therefore, in order to apply FEA, they need to be converted to STEP format, which is commonly utilised in Computer Aided Design (CAD) softwares. Function that transforms mesh to Non-Uniform Rational B-Spline (NURBS), which is available in certain CAD software, e.g. RhinoCAD, is used for conversion. This process is resource intensive and may cause a reduction in the specimen precision.

For the simulation experiment in ANSYS, the STEP files are imported to a native format for being meshed. Two types of material, according to the material powder for laser sintering, are assigned to the meshed models. Materials are Polyamide (PA2200) and Stainless Steel (GP1), where the properties are shown in Table 1.

Material	Density $g\,cm^{-3}$	Young's Modulus MPa	Poisson's Ratio	Tensile Yield Stress MPa	Compressive Yield Strength MPa
EOS PA2200	0.93	1700 1432*	0.4	48	48
EOS Stainless Steel	7.8	185000 26000*	0.305	530	530

Table 1: Material Properties from Literature (* from empirical test)

In order to simplify the experiment, a displacement was utilised instead of the application of a load to the specimen to avoid any form of artefacts or deformation in the simulation as a result of the loading steps. The deformation value is used to align the results from simulation and physical experiments.

3. Experiments

3.1. Design of experiment

From the family of Triply Periodic Minimalistic Surface (TPMS) algorithms, the three aforementioned types of cells were selected due to their maximised amounts of cell wall thickness between internal junctions and their symmetry. The Youngs modulus in material data sheet [13, 14] were found to be wildly inaccurate when actually tested. More accurate values for the elastic modulus were found through empirical testing, resulting in a youngs modulus of 1234.1 MPa (for PA2200) and 26 GPa (for GP1)(see Table 1).

Increasing the cell wall thickness increases the overall volume of the cellular structure. Due to this behaviour, by increasing the amount of material the load is transferred across is desired to be analysed. It should be noted that, a larger cell wall value results in a larger void area and therefore a smaller cross-sectional are of the cell walls.

In summary, the experiments are conducted according to the following variations: Unit Cell Wall length (6mm, 10mm), Material (PA2200, GP1), and Cell Wall thickness (0.6mm, 0.7mm). The unit cells in each case are tessellated to form a larger testing specimen, with cube length 18mm and 20mm.

To examine the material specimen response through physical tests, each specimen was compressed with variable increasing loads. The force was transferred to each structure through the top face. As the force was applied, the equipment recorded the stress and strain induced in each step.

3.2. Simulation Result

Fig.2 (a)-(f) show the displacement induced in FEA testing. All cell types exhibit similar behaviour, namely possessing the maximum displacement on the load-bearing face and the lowest at the supporting face, however they all exhibit different amounts of buckling on the edges. Fig.3 (a)-(f) show the superimposed results of the FEA load response of each cell type against the empirically tested specimens, showing the extremely large difference in youngs modulus between simulation and empirical testing.

3.3. Empirical Result

When comparing specimens with identical parameters - (a) cell wall thickness, (b) unit cell length, and (c) angle - while adjusting the material parameter of the test, it can be seen that the material with the higher elastic modulus performs much better in terms of yield strength. From the specimens, yield strength of stainless steel is much higher than PA2200 as the youngs modulus of stainless steel is 95% higher.

Regarding the buckling and failing of the specimens, the laser sintered specimens exhibited different characteristics. A large number of the specimens when empirically tested began to buckle and lean to one side (see Fig. 4c-e). Because there was, in general, no failure in the specimen, the compression test was continued. However, the buckling of the specimen may have had a large effect on the empirical data, as the force applied was no longer purely vertical across the specimen.

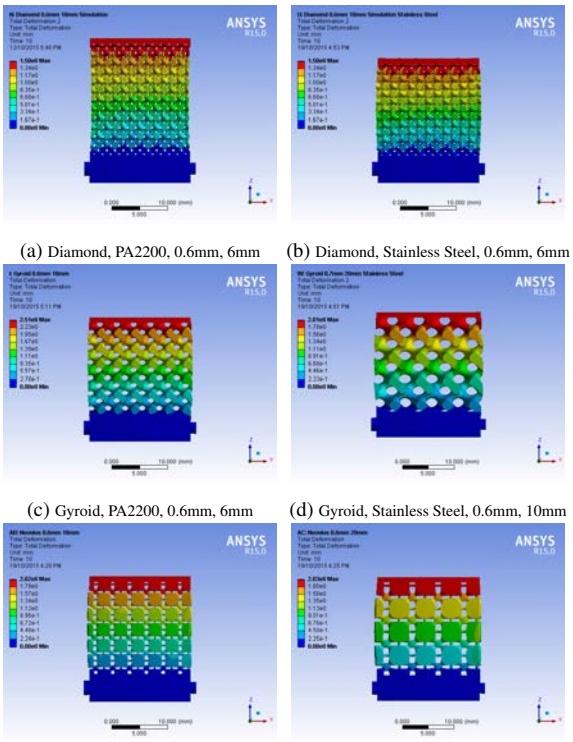

(a) Diamond, PA2200, 0.6mm, 6mm (b) Diamond, Stainless Steel, 0.6mm, 6mm

(c) Gyroid, PA2200, 0.6mm, 6mm (d) Gyroid, Stainless Steel, 0.6mm, 10mm

(e) Neovius, PA2200, 0.6mm, 6mm (f) Neovius, PA2200, 0.6mm, 10mm

Fig. 2: Deformation of specimens analysed in simulation (Type, Material, wall thickness (mm), unit cell length (mm))

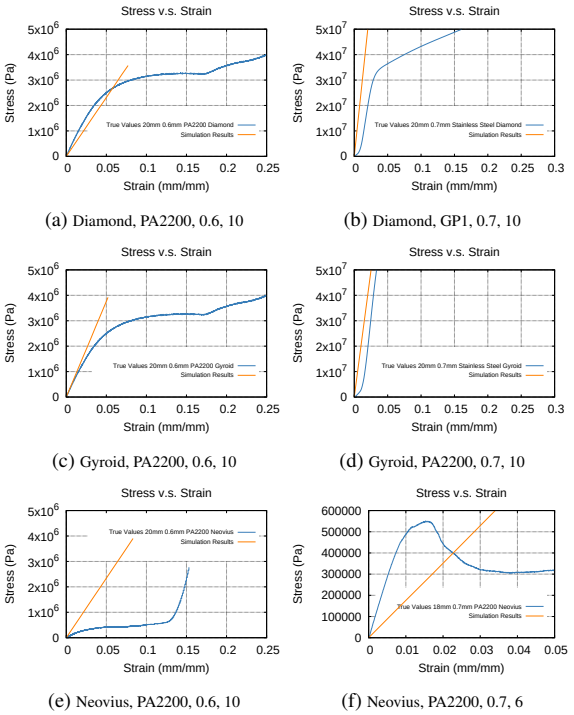

(a) Diamond, PA2200, 0.6, 10 (b) Diamond, GP1, 0.7, 10

(c) Gyroid, PA2200, 0.6, 10 (d) Gyroid, PA2200, 0.7, 10

(e) Neovius, PA2200, 0.6, 10 (f) Neovius, PA2200, 0.7, 6

Fig. 3: Stress Strain curve of specimens analysed in simulation (Type, Material, wall thickness(mm), unit cell length (mm))

From Fig. 4 (a)-(d), the Gyroid and Diamond structures after compression appear to deform in a shape similar to that shown in the deformation from the FEA simulation. They appear to buckle and feature a curve on the extremities that show the bowing of the cells induced by the downwards load applied to the top face. The Neovius structure (see Fig. 4 (c)-(d)), however, failed catastrophically as the compression test continued, as the cells were too small to resist the load.

3.4. Result Summary

From both experiment and simulation, the strongest cellular structure type as an average of yield stress is the Gyroid type, as it possesses a higher strength than the Diamond type. The Neovius cell type performed the worst, due to the thin cellular walls between layers and their inability to withstand any load, causing their yielding and buckling. Table 2 shows the experiment results where the parameters are varied. The error present in each specimen describes the ratio of actual youngs modulus found via empirical testing and the youngs modulus from FEA. A negative result means that the specimen is much weaker than simulated, whereas a positive result indicates that the empirical specimen is much stronger than computed.

4. Discussion

As seen in many specimens in Table 2, particularly in the Diamond with 0.7 mm wall thickness and 10 mm unit cell length specimen, the cellular structures sometimes exhibit a unique phenomenon which can be discussed in the following points:

4.1. Multiple yield points

As the yield point is passed and the specimen approaches its first ultimate compressive strength, the layer experiencing the largest amount of stress across the surface area of the layer will fail and buckle. This results in an extremely large drop in stress as the strain increases as the layer continues to fail. However, as the failed layer is compressed into the next layer, the strength increases again to a second yield point until it again fails and another layer fails. This process is continued until the cellular structure is sheared due to unsymmetrical buckling, or the specimen is compressed until the two non-cellular caps are touching. The result is primarily unwanted in this study, however this behaviour could specifically targeted to be utilised in a variety of ways, such as increasing the strength of a structure as it fails.

4.2. Porosity of materials

The modelling methods in software packages, e.g. ANSYS [16] and Nastran [17], assume that the specimen being analysed is homogeneous, which means the object is either cast or made by subtractive manufacturing. The issue with this extremely large assumption is that for porous materials such as polystyrene or wood, the finite element analysis method cannot account for uniform porosity. The material sample can differ in the distribution of the specimen voids creating localised areas that are susceptible to high stress and strain concentrations.

(a) Physical Test of PA2200 Diamond 0.6mm Cell Wall Thickness, 6mm Unit Cell Wall Length

(b) Physical Test of GP1 Diamond 0.6mm Cell Wall Thickness, 6mm Unit Cell Wall Length

(c) Physical Test of PA22200 Gyroid 0.6mm Cell Wall Thickness, 10mm Unit Cell Wall Length

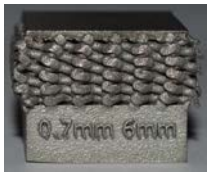

(d) Physical Test of GP1 Gyroid 0.7mm Cell Wall Thickness, 6mm Unit Cell Wall Length

(e) Physical Test of PA22200 Neovius 0.6mm Cell Wall Thickness, 6mm Unit Cell Wall Length

(f) Physical Test of PA2200 Neovius 0.7mm Cell Wall Thickness, 6mm Unit Cell Wall Length

Fig. 4: Physical Testing Results

Because the DMLS method does not reach the melting point of the material, it only compacts and forms the intended object. As a result, non-uniform distribution of voids possibly occurs between particles as the particles in powder do not form a continuous mass but instead are comprised of particles joined together at boundaries.

The findings are supported by a number of research works. [13] describes the porosity of the specimen as the cause of a 10% difference between the empirical and theoretical elastic modulus of Nylon 12, which is almost identical to PA2200. Their conclusions also corroborate our findings that the initial failure within a laser sintered component relates to pores and results in critical inaccuracy in modelling of compression. [14] and [18] include a porosity parameter in a numerical method in order to represent porosity in DMLS parts. In regard to our study, cellular structures include members having extremely small cross-sectional areas and the testing conditions were not controlled for uniformly controlled porosity percentage. Extremely large amount of error between empirical and theoretical testing was found.

An alternative to this issue of porosity is the utilisation of SLM or DLM instead of the DMLS method. The SLM and DLM method reaches the melting point of the metallic powder [19] and as such avoids the issue of non-uniform porosity distribution across the specimen. Theoretically, any specimens produced using the DLM method should perform better with a higher Young's Modulus and yield strength compared to identical specimens produced utilising DLMS.

Cell Type	Unit Cell Length (mm)	Cube Length (mm)	Cell Wall Thickness (mm)	Material	Youngs Modulus Empirical (Pa)	Youngs Modulus Simulation (Pa)	Error
Diamond	6	18	0.6	PA2200	3.52E+07	4.36E+07	-23.77%
Diamond	6	18	0.7	PA2200	1.54E+07	3.20E+07	-108.05%
Diamond	10	20	0.6	PA2200	5.74E+07	4.64E+07	19.25%
Diamond	10	20	0.7	PA2200	2.41E+06	8.10E+07	-3258.98%
Gyroid	6	18	0.6	PA2200	7.21E+07	1.36E+07	81.14%
Gyroid	6	18	0.7	PA2200	4.86E+07	6.20E+07	-27.57%
Gyroid	10	20	0.6	PA2200	5.60E+07	7.53E+07	-34.48%
Gyroid	10	20	0.7	PA2200	3.73E+07	6.35E+07	-70.12%
Diamond	6	18	0.6	GP1	2.22E+09	1.29E+09	41.85%
Diamond	10	20	0.7	GP1	1.51E+09	2.48E+09	-64.03%
Gyroid	6	18	0.7	GP1	2.42E+09	1.85E+09	23.44%
Gyroid	10	20	0.7	GP1	2.23E+09	1.99E+09	10.62%
Neovius	6	18	0.6	PA2200	7.29E+06	4.00E+07	-448.79%
Neovius	6	18	0.7	PA2200	5.52E+07	1.76E+07	68.13%
Neovius	10	20	0.6	PA2200	1.40E+07	4.68E+07	-234.25%

Table 2: Result Summary - Physical and Simulation

4.3. Force

Regarding to the non-porous material assumption, the FEA solver applied forces across the axis parallel to the laser sintering manufacturing direction and assumed that there was no force induced in other directions. In reality, the forces applied during the compression testing relied on the nature of the specimen, for example force dispersing along the particle bonding boundaries (see Fig. 5(a)). As can be seen, theoretically the forces will be applied across all axes instead of the simulated single axis. Consequently, unavoidable errors are induced directly proportional to the amount of porosity in the sample. To further avoid the issue of non-vertical forces, a jig can be manufactured and utilized during compression testing to encompass the specimen being tested in order to avoid the boundaries having non-vertical forces exerted on them, in an attempt to unify the direction of force applied from the compression testing die. The application of such a solution could prevent premature yielding issues, as seen in the 35 degree laser sintered manufactured specimens, which caused extreme yielding and shearing of the specimens.

4.4. Imperfection in material powder and manufacturing

Fig. 5(b) shows that the particles in the laser sintering powder are not perfectly spherical and non-uniformly distributed. These issues cause a sporadic connection between particles and further exacerbate the force transfer issue. In addition, a potential cause of the error is the reproduction of curved surfaces during laser sintering. The curve surfaces can reduce stress concentration on the sharp corner. However, producing the required curve surface on the specimens with small cellular wall thickness, 0.6 - 0.7mm, may be impossible.

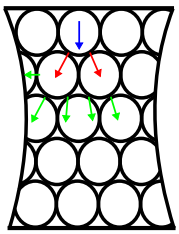

(a) Distributon of force within specimen

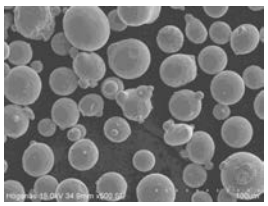

(b) Scanning Electron Microscope capture of non-homogeneous distribution of powder

Fig. 5: Particles of Material Powder

5. Conclusions

As discussed in previous section, for a variety of factors outlined in this study, the simulation of cellular structures produced through the laser sintering manufacturing method is not viable. Since the errors calculated through the comparison of the experimental and simulated Young's Modulus and yield strength are extremely high for most specimens, it can be concluded that the FEA model does not converge to a solution that approximates the empirical testing data.

It was shown through a variety of further testing that the non-convergent solutions of the simulated tests to the empirical data were caused by the non-uniform distribution of porosity within the specimen. This phenomenon leads to the error of the simulation as the commercial FEA products are unable to accurately solve non-solid object models. It is therefore evident that cellular structures do not follow usual material properties that are assumed in traditional FEA and hence existing theories fail when applied.

6. Future Work

Custom micro-molecular FEA modelling software could be developed to achieve greater accuracy when testing Direct Metal Laser Sintered manufactured parts. Although numerical FEA solvers are currently available, they are limited in application and not intended to be utilised with cellular structures.

There is also a wide scope of research that could be investigated in order to explain the structural behaviour of the cellular structures, including the multiple yield phenomenon, which could be the basis of a new field of research.

7. Acknowledgement

We would like to thank Advanced Manufacturing Services, Breseight Pty Ltd, Australia, for building experimental specimens.

References

[1] Shellabear, M., Nyrhilä, O.. Dmls Development History and State of the Art. Lane 2004 2004;:1–12.

[2] Yan, C., Hao, L., Hussein, A., Raymont, D.. Evaluations of cellular lattice structures manufactured using selective laser melting. International Journal of Machine Tools and Manufacture 2012;62:32–38. doi:10.1016/j.ijmachtools.2012.06.002.

[3] Pasko, A., Vilbrandt, T., Fryazinov, O., Adzhiev, V.. Procedural function-based spatial microstructures. SMI 2010 - International Conference on Shape Modeling and Applications, Proceedings 2010;:47–56doi:10.1109/SMI.2010.19.

[4] Qiu, L., Liu, J.Z., Chang, S.L.Y., Wu, Y., Li, D.. Biomimetic superelastic graphene-based cellular monoliths. Nature communications 2012;3:1241. doi:10.1038/ncomms2251.

[5] Rehme, O., Emmelmann, C.. Rapid manufacturing of lattice structures with Selective Laser Melting. Laser-based Micropackaging 2006;6107:61070K–61070K–12. doi:10.1117/12.645848.

[6] Hussein, A., Hao, L., Yan, C., Everson, R., Young, P.. Advanced lattice support structures for metal additive manufacturing. Journal of Materials Processing Technology 2013;213(7):1019–1026. doi:10.1016/j.jmatprotec.2013.01.020.

[7] Scheffler, M., Colombo, P.. Cellular Ceramics: Structure, Manufacturing, Properties and Applications. Wiley; 2006. ISBN 9783527606702.

[8] Brooks, W., Sutcliffe, C., Cantwell, W., Fox, P., Todd, J., Mines, R.. Rapid design and manufacture of ultralight cellular materials. Solid Freeform Fabrication Symposium 2005;:231–241.

[9] Wang, H., Chen, Y., Rosen, D.W.. A Hybrid Geometric Modeling Method for Large Scale Conformal Cellular Structures. 25th Computers and Information in Engineering Conference, Parts A and B 2005;3:421–427. doi:10.1115/DETC2005-85366.

[10] Vongbunyong, S., Kara, S.. Selective volume fusing method for cellular structure integration. In: Sustainability Through Innovation in Product Life Cycle Design, Proceedings of EcoDesign 2015 International Symposium. 2015, p. 508–513.

[11] Vongbunyong, S., Kara, S.. Rapid generation of uniform cellular structure by using prefabricated unit cells. International Journal of Computer Integrated Manufacturing 2016;.

[12] Hao, L., Raymont, D., Yan, C., Hussein, A., Young, P.. Design and additive manufacturing of cellular lattice structures. In: Innovative Developments in Virtual and Physical Prototyping, Proceedings of the 5th International Conference on Advanced Research in Virtual and Rapid Prototyping, Leiria, Portugal. 2012, p. 249–254.

[13] Ajoku, U., Hopkinson, N., Caine, M.. Experimental measurement and finite element modelling of the compressive properties of laser sintered Nylon-12. Materials Science and Engineering 2006;428(1-2):211–216. doi:10.1016/j.msea.2006.05.019.

[14] Shen, H., Oppenheimer, S.M., Dunand, D.C., Brinson, L.C.. Numerical modeling of pore size and distribution in foamed titanium. Mechanics of Materials 2006;38(810):933–944. doi:http://dx.doi.org/10.1016/j.mechmat.2005.06.027.

[15] The MathWorks, I.. MATLAB 8.0 and Statistics Toolbox 8.1. 2012.

[16] ANSYS Academic Research, . ANSYS Structures. 2013.

[17] MSC Software, . Nastran. 2013.

[18] Shen, H., Brinson, L.. Finite element modeling of porous titanium. International Journal of Solids and Structures 2007;44(1):320–335. doi:10.1016/j.ijsolstr.2006.04.020.

[19] Kruth, J., Froyen, L., Van Vaerenbergh, J., Mercelis, P., Rombouts, M., Lauwers, B.. Selective laser melting of iron-based powder. Journal of Materials Processing Technology 2004;149(1-3):616–622. doi:10.1016/j.jmatprotec.2003.11.051.